



Contents lists available at ScienceDirect

Science of the Total Environment

journal homepage: www.elsevier.com/locate/scitotenv

Global land-use allocation model linked to an integrated assessment model

Tomoko Hasegawa^{a,b,*}, Shinichiro Fujimori^{a,c}, Akihiko Ito^d, Kiyoshi Takahashi^a, Toshihiko Masui^a

^a Center for Social and Environmental Systems Research, National Institute for Environmental Studies (NIES), 16-2 Onogawa, Tsukuba, Ibaraki 305-8506, Japan

^b Ecosystem Services and Management Program, International Institute for Applied Systems Analysis (IIASA), Laxenburg A-2361, Austria

^c Energy Program, International Institute for Applied Systems Analysis (IIASA), Laxenburg A-2361, Austria

^d Center for Global Environmental Research, National Institute for Environmental Studies (NIES), 16-2 Onogawa, Tsukuba, Ibaraki 305-8506, Japan

HIGHLIGHTS

- Development of a global land-use allocation model to be linked to integrated assessment models (IAMs).
- Description of the developed model and model evaluation for the estimated land-use allocation.
- Downscaling of the IAMs' regional land-use projections into a spatial land-use distribution.
- Illustration of influences of land-use downscaling on estimates of CO₂ emissions from land-use changes.

ARTICLE INFO

Article history:

Received 23 September 2016

Received in revised form 3 December 2016

Accepted 3 December 2016

Available online xxxxx

Editor: D. Barcelo

Keywords:

Land-use change

Spatial allocation

Integrated assessment

ABSTRACT

We developed a global land-use allocation model that can be linked to integrated assessment models (IAMs) with a coarser spatial resolution. Using the model, we performed a downscaling of the IAMs' regional aggregated land-use projections to obtain a spatial land-use distribution, which could subsequently be used by Earth system models for global environmental assessments of ecosystem services, food security, and climate policies. Here we describe the land-use allocation model, discuss the verification of the downscaling technique, and explain the influences of the downscaling on estimates of land-use carbon emissions. A comparison of the emissions estimated with and without downscaling suggested that the land-use downscaling would help capture the spatial distribution of carbon stock density and regional heterogeneity of carbon emissions caused by cropland and pasture land expansion.

© 2016 Published by Elsevier B.V.

1. Introduction

Land use and land-use changes involve interactions between human activities and natural systems. For example, deforestation, agriculture and bioenergy may affect ecosystems, water resources, biodiversity, and the climate system, whereas these biophysical systems may change human activities, decision making and the environment. Many stand-alone land-use models (LUMs) and land-use modules as a part of integrated assessment models (IAMs) have been developed with different modeling approaches, scales and resolutions, such as CAPS (Meiyappan et al., 2014), CLUEMondo (van Asselen and Verburg,

2013), GCAM (Wise and Calvin, 2011), GLOBIOM (Havlík et al., 2011), GLM (Hurtt et al., 2006), IMAGE (Letourneau et al., 2012), LandSHIFT (Schaldach et al., 2011), MAgPIE (Lotze-Campen et al., 2010), the Nexus land-use model (Souty et al., 2012), the Land-Use Trade-Offs (LUTO) model (Bryan et al., 2016) and so on. To understand uncertainty, difference in land cover projections were investigated in several approaches (Alexander et al., 2016; Gao et al., 2016). For instance, the difference in a wide range of model types and scenarios shows a higher degree of uncertainty in land-use projections than that in climate or earth system projections. This analysis raised as a future challenge better understanding the assumptions driving land use model results and to reveal the causes of uncertainty in more depth to help reduce model uncertainty and improve the land cover projections.

Recently, an integration of Earth system models (ESMs) and IAMs has been increasingly needed for addressing the issues that are driven by integrative biogeophysical, socioeconomic and human decision-making perspectives (Bond-Lamberty et al., 2014; Hibbard et al.,

* Corresponding author at: Center for Social and Environmental Systems Research, National Institute for Environmental Studies (NIES), 16-2 Onogawa, Tsukuba, Ibaraki 305-8506, Japan.

E-mail address: hasegawa.tomoko@nies.go.jp (T. Hasegawa).

2010). The collaboration of the two communities is expected to play an important role and to help better understand the role of both natural and human systems and their interaction. The ESMs capture geophysical aspects such as climate, global carbon cycle, terrestrial vegetation, and ocean ecosystem whereas the IAMs have focused on socio-economic aspects such as energy, economic systems, and associated greenhouse gas emissions and considered land use as a fundamental factor to produce agricultural and forest products. However, in the integration, there is a gap between their regional classifications. The ESMs have a grid-based spatial resolution, whereas most of the IAMs have aggregated regional divisions. To promote the integration, there is a need for downscaling of the socioeconomic, emission and land-use scenarios projected by IAMs. Hibbard et al. (2010) and van Vuuren et al. (2010) raise transparency and consistency as criteria of downscaling methodologies and requires diagnostics using different downscaling methods against historical data. Some land use models have been evaluated at country or regional scale (e.g. Kok et al., 2001), but global-scale evaluation is still limited due to data issues (Meiyappan et al., 2014). The model evaluation method presented here could be provided as an example for a global-scale model evaluation. Moreover, global-scale evaluation is important for better understanding of the role of land dynamics in global changes. Although an evaluation of model performance over the historical period does not necessarily guarantee a good performance for future, a high agreement of historical patterns provides information about the uncertainty of future scenarios for the global environmental assessment.

In this study, we developed a land-use allocation model that works with an IAM: the Asian-Pacific Integrated Model/Computable General Equilibrium (AIM/CGE) model. To determine the uncertainty of estimated land-use patterns, we performed verification for a downscaling methodologies by applying the model to a historical period (see Section 2.2 for more detail). Moreover, we conducted a downscaling of aggregated land-use scenarios estimated by AIM/CGE into the gridded level using the model, and investigated the influences of the downscaling on estimates of land-use emissions.

2. Materials and methods

2.1. Land-use allocation model

2.1.1. Mechanism of land-use allocation

Fig. 1 shows the overall framework of the methodology. Regional aggregated land demand projected by AIM/CGE (17 regions) was fed into the land-use allocation model and was downscaled into grid cells (0.5° × 0.5°). The cropland and afforestation area was allocated based on profit maximization where a land owner would decide land-use sharing to obtain the highest profit under a given biophysical land productivity (production per unit area). Since this process was conducted in each region and grid cell, land transactions across the regions were not allowed. The allocation was conducted in 5-year steps. There were seven crop types, with or without irrigation (Table 1). The crop types were aggregated as cropland for model verification according to the availability of historical cropland data. Land for wood production was excluded from this work. To convert quantities of harvested wood into areas of land, information regarding the historical map of harvested aboveground biomass, and the subsequent recovery following wood harvesting and land-use abandonment are needed. However, no global, gridded, or historical record of these data are available (Hurt et al., 2011).

2.1.2. Formulation

The following formulas refer to a certain year and region. The upper bars represent exogenous parameters.

Total profit was maximized as follows:

$$\Phi = \sum_{l,g} Z_{l,g} \rightarrow \text{Max.} \tag{1}$$

where g is a set of grid cells, l is a set of land-use categories, Φ is total profit (million US\$), and $Z_{l,g}$ is the profit of land-use category l in grid cell g (million US\$).

The profit was represented as profit (S) minus land conversion cost ($a_{l,g}$) as shown in Eq. (2). The second term accounts for the land conversion cost by multiplication with the increase in the fractional area of land-use from the previous year ($\Delta Y_{l,g}$). For this calculation, land-use patterns in the previous year were fed into the next year's calculation.

$$Z_{l,g} = \left(Y_{l,g} \cdot \overline{S_{l,g}} - \overline{a_{l,g}} \cdot \Delta Y_{l,g} \right) \cdot \overline{GA_g}, \quad g \in G, l \in L \tag{2}$$

Subject to

$$Y_{l,g} - \overline{Y_{pre_{l,g}}} = \Delta Y_{l,g} - \Delta YN_{l,g} \tag{3}$$

where $Y_{l,g}$ is the fractional area of each land-use category l in grid cell g (grid⁻¹), $S_{l,g}$ is profit per area (million US\$/ha), $a_{l,g}$ is land conversion cost per area (million US\$/ha), GA_g is grid cell area (ha/grid), $Y_{pre_{l,g}}$ is the fractional area in the previous year (grid⁻¹), $\Delta Y_{l,g} (>0)$ is the increase in the fractional area from the previous year (grid⁻¹), and $\Delta YN_{l,g} (>0)$ is the decrease in the fractional area from the previous year (grid⁻¹).

The fractional area should not be negative:

$$Y_{l,g} \geq 0, \quad g \in G, l \in L \tag{4}$$

The total fractional area in a grid cell should be equal to or less than 1:

$$\sum_l Y_{l,g} \leq 1, \quad g \in G, l \in L \tag{5}$$

For each land-use category, the total area of land allocated should meet the given land demand area LDM_l :

$$\sum_g \overline{GA_g} \cdot Y_{l,g} = \overline{LDM_l}, \quad l \in L \setminus \{hav, frs\} \tag{6}$$

where LDM_l is the land demand area (exogenous) for land-use category l (ha/year).

Other land-use is defined as:

$$Y_{oth',g} = 1 - \sum_{l \neq oth} Y_{l,g} \tag{7}$$

where $Y_{oth',g}$ is the fraction of grid cell area in other land-use categories (forest, pasture, and other natural vegetation).

To avoid land conversion of the protected area, the fractional area of other land (OTH), including forest, was assumed to be more than the fraction of protected area:

$$Y_{oth',g} \geq \overline{Y_{protect_g}} \tag{8}$$

where $Y_{protect_g}$ is the fraction of protected area in grid cell g (grid⁻¹).

Assuming that human activity does not expand into areas with extremely low population density (Klein Goldewijk et al., 2011), cropland and afforestation were not allocated in areas with a density of less than 0.1 person/km²:

$$Y_{oth',g} = 1 \quad \text{if } popd_g < 0.1 \tag{9}$$

where $popd_g$ is the population density (person/km²).

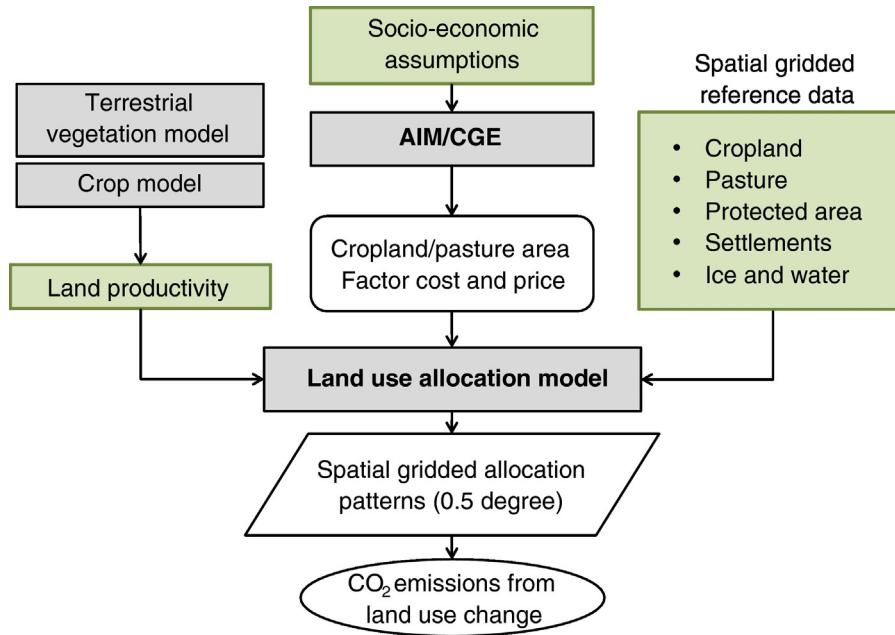


Fig. 1. Overall framework of the land-use allocation methodology.

Afforestation was assumed in non-forest areas with a carbon stock density lower than 2 kgC/m², which was used as a definition, based on the carbon stock density, to differentiate forest and non-forest areas in Hurtt et al. (2011):

$$Y_{aff,g} = 0 \quad \text{if} \quad CS_g > 20 \quad (10)$$

where $C S_g$ is the mean carbon stock density in grid cell g (MgC/ha).

2.1.3. Allocation of pasture, forest, and other natural vegetation

Potential profit from livestock products is determined by livestock intensity and productivity which are determined by livestock species,

feed requirement, and farming systems and types (Havlík et al., 2014). Since there is no sufficient data for estimating future distribution of potential profit from livestock products, pasture land was simply expanded or shrunk by scaling the base-year distribution up or down to meet the demand of pasture area. The pasture area was allocated to areas unprotected and unused for crop production and afforestation (see Section S2 of Supplementary material for more detail.). Then, forest and other natural vegetation were allocated on other land (OTH), excluding pasture, according to the carbon stock density in each grid cell. A level of carbon stock density between forest and grassland was determined so that the forest area was the same as the statistically determined forest area.

2.1.4. Carbon emissions and changes in carbon stock density

Carbon emissions from forest conversions were calculated from changes in the land use area and carbon stock density, while the carbon sink in afforestation areas was calculated from the area of afforestation ($YT_{l,g,t}$) and annual biomass growth ($CFT_{g,t,t'}$) (Eq. (11)). We used a timber yield function (Sohngen et al., 2009) to determine the changes in annual biomass growth according to forest age.

$$\Delta C_{l,g,t} = \begin{cases} -CS_{l,g} \cdot \Delta Y_{l,g,t} \cdot GA_g, & l = CL, PAS, FRS, ONV \\ \sum_{t' \text{ if } t_{base} \leq t' \leq t} -CFT_{g,t,t'} \cdot YT_{l,g,t'} \cdot GA_g & l = AFR \end{cases} \quad (11)$$

Eq. (11) is subject to:

$$\Delta Y_{l,g,t} = Y_{l,g,t} - Y_{l,g,t-1}$$

where $\Delta C_{l,g,t}$ is the carbon emission (positive values) and sink (negative values) in land category l , grid g , in year t (MgC/grid/year), $CS_{l,g}$ is the carbon stock density in land category l , grid cell g in year t (MgC/ha), $CFT_{g,t,t'}$: is the annual biomass growth ratio of forest planted in year t' in grid g , year t , (MgC/ha/year), $\Delta Y_{l,g,t}$ is the change in fractional area in land category l , grid g in year t (year⁻¹), and $YT_{l,g,t}$ is the fractional area in land category l , grid g in year t (grid⁻¹).

The carbon stock density changed with changes in the land-use pattern every year as shown in Eq. (12). For example, cropland expansion

Table 1 Land-use categories included in the land-use allocation model.

Categories (l)		Code	Future estimation	Model verification
Cropland	Rice irrigated	CL	PDRIR	X
	Wheat irrigated		WHTIR	X
	Other coarse grains irrigated		GROIR	X
	Oil crops irrigated		OSDIR	X
	Sugar crops irrigated		C_BIR	X
	Rice rainfed		PDRRF	X
	Wheat rainfed		WHTRF	X
	Other coarse grains rainfed		GRORF	X
	Oil crops rainfed		OSDRF	X
	Sugar crops rainfed		C_BRFR	X
	Other crops		OTH_A	X
	Bioenergy crops	BIO		X
	Afforestation		AFR	X
Settlement		SL	X	X
Ice and water		OL	X	X
Other land-use		OTH	X	X
	Forest		FRS	X
	Pasture		PAS	X
	Other natural vegetation		ONV	X

decreased the carbon stock, while afforestation increased the stock. Carbon emissions/sinks and changes in carbon stock density were calculated every year as a post process. Then the carbon stock in the previous year is fed into the next year.

$$CS_{g,t+1} = \frac{CS_{g,t} \cdot GA_g - \sum_l \Delta C_{l,g,t}}{GA_g} \quad (12)$$

2.1.5. Parameter settings and data used

1) Profit and land conversion cost

The two main parameters in Eq. (2) are profit (S) and land conversion cost (a). Profit was defined as revenue minus cost. Revenue from crop production was the multiplication of crop price and yield. Revenue from afforestation included revenue from the carbon sequestration of the forest and the benefits of forest restoration. Cost for crop production and afforestation were calculated by a total sum of capital, labor, and intermediate costs divided by the land area for the according sectors. This cost and land area information was provided by AIM/CGE, and was uniformly used for the grids in each region.

The land conversion cost included road construction costs, irrigation cost, and payments for land-use emissions (Eq. (14)). Road construction costs were derived from road length and the construction cost per unit length (WorldBank, 2014). Road length included i) rural road length (IRF, 2009) and ii) the distance from the nearest grid occupied by the same land category which represents neighborhood effects in land transition (Verburg et al., 2004). Irrigation costs were obtained from multiplying the irrigated area and the cost per unit irrigated area (Nelson et al., 2009). The costs of carbon emission were considered in mitigation scenarios, where a price was placed on carbon (see Section S3 of Supplementary material for more detail).

2) Land productivity and carbon stock density

The mean crop yields of the irrigated or rain-fed area were calculated using data for the period 1990–2004 from the Lund-Potsdam-Jena managed Land Dynamic Global Vegetation and Water Balance Model (LPJmL), provided by the Inter-Sectoral Impact Model Intercomparison Project (ISIMIP) (Rosenzweig et al., 2014). The yields of 13 crops, as determined by the LPJmL were aggregated into the seven crop classifications of the model for each grid cell using the crop production of the country which the grid cell belonged to (FAO, 2013), as a weighting. All of the crop yields considered CO₂ fertilization.

For the base-year carbon stock density and energy-crop yields, we used estimates from a process-based biogeochemical model (the Vegetation Integrative Simulator for Trace gases; VISIT) (Ito and Inatomi, 2012). The annual biomass growth ratio was changed with forest age using a timber yield function (Sohngen et al., 2009). A parameter of the timber yield function was estimated by assuming the potential carbon stock density as a saturated level. For the potential carbon stock density, we referred to the carbon stock density for Agro-Ecological Zones (AEZs) (IPCC, 2006), and allocated the density to grids according to the AEZ of each grid.

3) Reference land-use map

For the reference land-use distribution used in the base-year allocation, cropland maps (Monfreda et al., 2008) were produced by aggregating 175 crop types into the crop classifications of the model (see Table S1 in Supplementary material for crop classifications). Representative concentration pathway (RCP) scenarios (Hurt et al., 2011) were used for settlements, ice, or water while United Nations Environment Programme–World Conservation Monitoring Centre (UNEP-WCMC, 2015) data were used for protected land. The base year irrigation ratio was calculated by multiplying a gridded current irrigation ratio (MIRCA2000) and the cropland ratio by crops (Monfreda et al., 2008). In cases where there was an inconsistency in land area among different data sources, land other than cropland and pasture was changed at the

same ratio so that total area was equal to country/regional land area. Then settlements, ice or water, and protected areas were assumed to be constant for the entire period.

2.2. The AIM/CGE model

The AIM/CGE model builds on the work by (Fujimori et al., 2012), and has been widely used for climate change studies (Hasegawa et al., 2015, 2016). In the model, supply, demand, trade, and investment are described as individual behavioral functions that respond to changes in the price of production factors and commodities, as well as changes in technology. The functions also respond to preference parameters on the basis of the assumed population, GDP, and consumer preferences. The model contains 17 regions and 42 industrial classifications including 10 agricultural sectors. Production functions are formulated as multinested constant elasticity substitution (CES) functions where land is a production factor for agricultural and forest commodities. Allocation of land by sectors is formulated as a multinomial logit function to reflect differences in substitutability across land categories with land rent (Fujimori et al., 2014). See Section S1 of the Supplementary material for more details about the CGE model and parameter settings.

We used baseline and mitigation scenarios generated by AIM/CGE. Both scenarios were based on shared socioeconomic pathway 2 (SSP2) assumptions. In the baseline scenario, no explicit climate mitigation was considered, while the mitigation scenario was defined by a radiative forcing in the year 2100 of 2.6 W/m². Fig. 2 shows the land-use change in the two scenarios. The area of forest and biomass crops decreased in the baseline scenario and increased in the mitigation scenario.

2.3. Model verification

2.3.1. Methods of model verification

To evaluate how different an allocation mechanism is from existing studies, we performed model verification in the period 1960–2005 as shown in Fig. 3. The existing data of regional land-use area were input to the model in 5-year steps, and then model's agreement was evaluated by comparing our estimates with the existing data in terms of spatial land-use distribution and CO₂ emissions. The consistency between the two values in spatial land distributions was evaluated using root mean squared error (RMSE), which represents the differences in the two spatial distributions.

Due to the limited availability of historical data regarding the spatial distribution of land-use, the model verification was conducted for two land categories: cropland and pasture. To evaluate the forest spatial allocation, we also compared land-use emissions with reported values (Smith et al., 2014) due to the limited data regarding historical forest distribution.

2.3.2. Data used for model verification

1) Crop yields and carbon stock density of forest

For crop yields, we used the mean yields of five crops (rice, wheat, other coarse grains, oil crops, and sugar crops) for the 1990s estimated by the Global Agro-Ecological Zones (GAEZ) model (Masutomi et al., 2009), in which this historical period was available (see Fig. S3). The yields of 13 types of crops were aggregated in each grid using the crop production of the country (FAO, 2013) to which the grid cell belonged as a weighting. The irrigation area was fixed at the present level (MIRCA2000) for the study period. For the carbon stock density and energy-crop yields, we used the estimates of the VISIT as shown above.

2) Land-use map and costs

Three types of land-use data were required for the model verification: regional aggregated land-use data as an input to the model, a reference land-use map for the base-year calculation, and the land-use map of existing studies for comparison. Data from Ramankutty (2012)

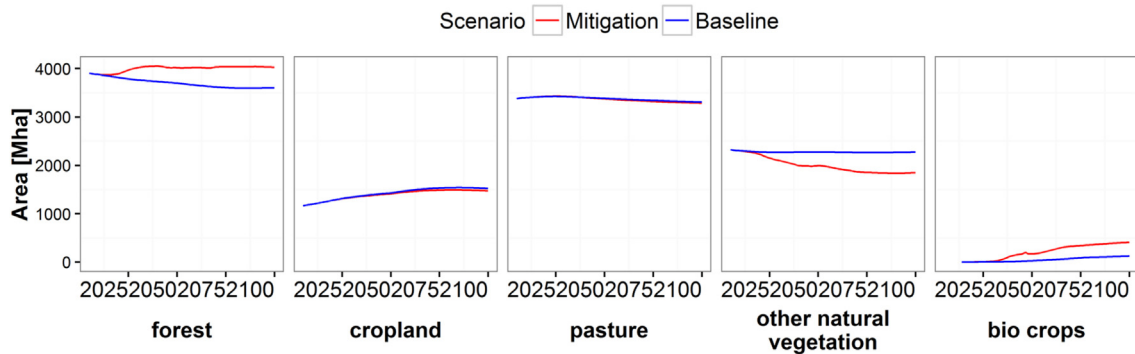


Fig. 2. Land-use area by categories estimated by the Asian-Pacific Integrated Model/Computable General Equilibrium (AIM/CGE).

were used for these three cases. The land-use map was aggregated at the regional level and fed into the model (Fig. S4). The land-use map in 1960 was used for reference in the base year of 1960, while the data from 1961 to 2005 was used for comparison with the model output. Profit and costs were fixed at the current level due to limited data availability.

3. Results

3.1. Model verification

Fig. 4 shows the RMSE representing mean differences in the area fractions in grids. The RMSE was 0.18/grid for cropland and 0.11/grid for pasture land at the global scale in 2005. There were two notable features in these differences. First, the differences increased over time and were relatively large in cropland compared to pasture land. Second, the differences were large in regions, particularly in aggregated regions, with a large historical change in cropland area (Oceania, Southeast Asia, the former Soviet Union [FSU], North Africa, Sub-Saharan Africa, and the Middle East). There was a large difference in countries with a large area and a large change in cropland areas (e.g., Brazil).

Fig. 5 show the discrepancy between our estimates and the existing reconstructed values of the fractions of cropland for selected years (see Fig. S5 for the spatial distribution of cropland and pasture land in 1960 and Fig. S6 for the discrepancy for pasture). Although the distribution is comparable with the reconstruction across the world, in some regions cropland was estimated to expand to high-yield areas over time (see Fig. S3 for yield distribution), resulting in differences with the existing cropland and pasture land data. This phenomenon was clearly seen in

the northeast coastal area of Australia, South Africa, and Brazil. This means that some of the reported pasture area, with potentially high crop yields, was selected as cropland as a result of model optimization, which led to differences with the reported data. This suggests that some areas with highest yields were not necessarily selected as cropland, and there might be some factors affecting cropland selection that were not considered.

3.2. Comparison of historical land-use emissions

Because the given land-use area was spatially distributed into grids, one way to evaluate agreement would be to compare land-use carbon emissions with existing studies. Fig. 6 compares the land-use emissions estimated in this study with existing studies reported in the Intergovernmental Panel on Climate Change Fifth Assessment Report (IPCC AR5) (Smith et al., 2014). Some studies included wood harvesting, forest degradation, and shifting cultivation, which were not included in this study. Emissions from peat lands were not considered here. With the exception of some regions and years, the estimations at the global scale and in the five regions considered in this study were within the range of existing studies. With a similar regional distribution, emissions in Asia and Latin America (LAM) were relatively large among the five regions. Global emissions were reported to be 3.3 GtCO₂eq/year (0.2–6.8 GtCO₂eq/year) in the 2000s, while this study estimated a value of 3.3 GtCO₂eq/year. However, on a regional basis, this study estimated lower values than the existing studies in LAM and Asia. In the 1980s in LAM, the Fifth Assessment Report (AR5) gave a value of 1.9 GtCO₂eq/year (0.9–2.75 GtCO₂eq/year), while this study estimated 0.44 GtCO₂eq/year. In the 1990s in Asia, the AR5 report gave a value of

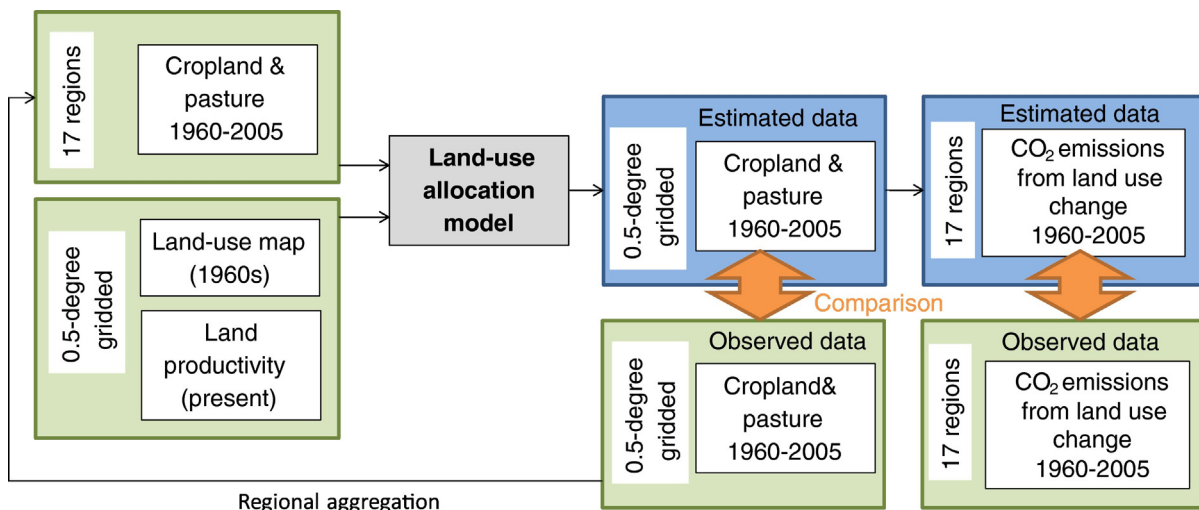


Fig. 3. A verification method for the estimated land-use allocation.

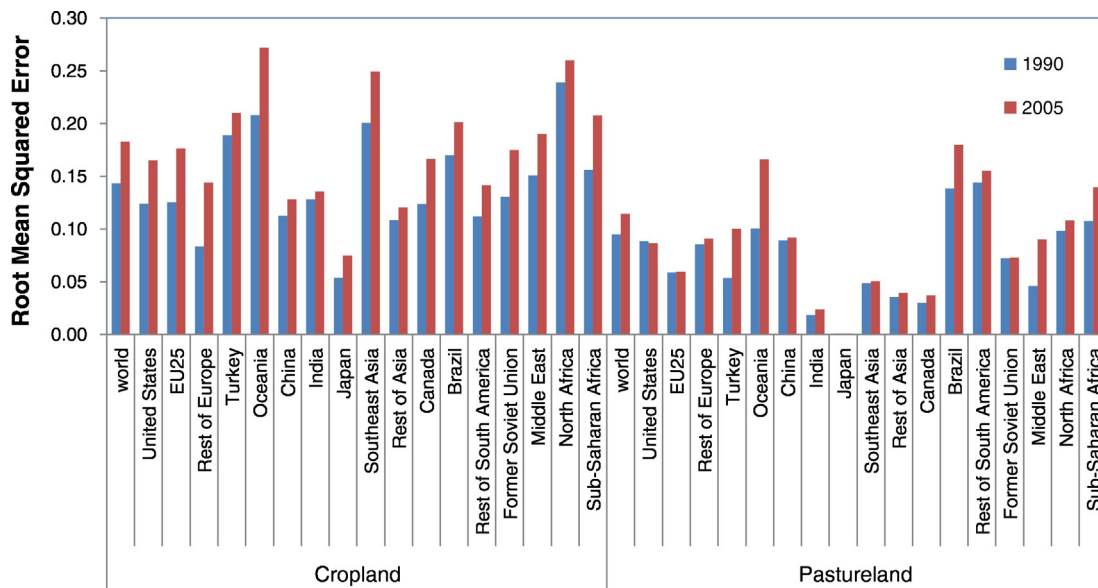


Fig. 4. Results of model verification, showing discrepancy of this study's estimates from the existing values for 1990 and 2005.

1.49 GtCO₂eq/year (0.85–1.95 GtCO₂eq/year), while this study estimated 0.62 GtCO₂eq/year.

One of the reasons for the differences can be the historical land-use datasets. There are mainly two historical datasets of global land-use distribution; (Ramankutty and Foley, 2010) (updated by Ramankutty, 2012) and HYDE3.1 (Klein Goldewijk et al., 2011). For the verification, we used Ramankutty (2012) for two reasons. First, it included annual data, while HYDE3.1 was decadal data. Second, it contained the latest available data, covering up to the year 2007. It should be noted that

these two historical datasets were constructed, not observed, and contained differences due to the different approaches and data used. For example, the decrease in pasture area after the 1980s reported in Ramankutty (2012) was likely the main reason for the differences in emissions in LAM shown in Fig. 6. Ramankutty (2012) reported that the pasture area decreased by 0.4 million ha from 1980 to 2005, whereas the FAO and HYDE3.1 reported that the pasture area increased by 42 and 41 million ha, respectively, in the same period. Most studies cited in AR5 use HYDE3.1 or Hurtt et al. (2011), which is based on HYDE3.1,

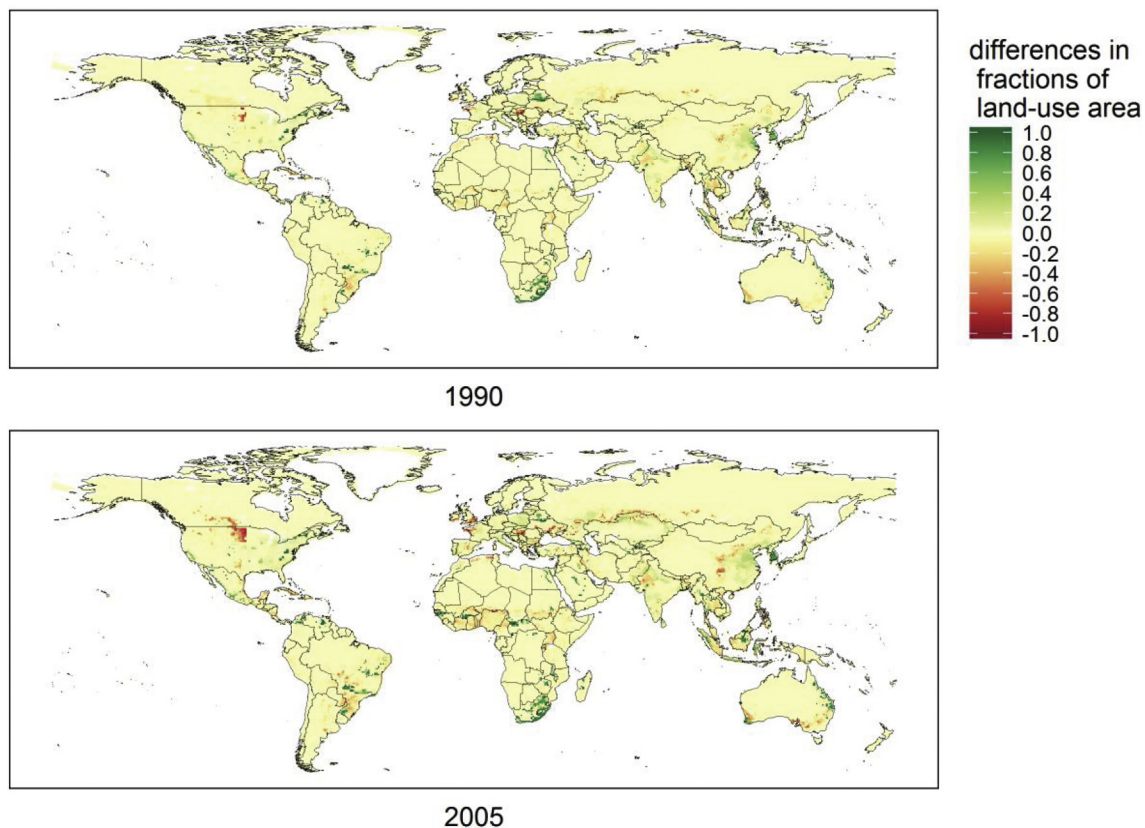


Fig. 5. Discrepancy in the fractions of grid cell area occupied by cropland of this study's estimations from the existing values in 1990 and 2005.

excluding Houghton (2012) and Jain et al. (2013) which used FAO and the three datasets (FAO, HYDE3.1, and Ramankutty), respectively. These differences in data sources for historical land-uses were likely to have produced the differences in the estimated emissions.

3.3. Downscaling land-use scenarios from an economic model

Figs. 7 and 8 show the changes in the fraction of land-use area from the base year for the baseline and mitigation scenarios, respectively (see Fig. S7 for the base-year spatial distribution of land-use). In the baseline scenario, cropland and pasture land expanded in sub-Saharan Africa, the eastern coastal area of Australia, and the east side of the United States, whereas the area of both land types shrank in China and the FSU. Afforestation expanded in the west of the FSU and the south of China. In sub-Saharan Africa, cropland for coarse grains, potatoes, and cassava expanded in the central area, while pasture land expanded over the entire area. In the east of the United States, cropland for maize and oil crops expanded, while in the east of Australia wheat fields expanded. In contrast, the area of cropland for potatoes and cassava shrank in the south of China, while the area of cropland for maize and wheat shrank in the central and west of the FSU.

In the mitigation scenario, more land was used for afforestation and bio crops compared to the baseline scenario. For example, in Brazil and FSU, there was an approximately 100 million ha larger area of afforestation in 2100 compared to the baseline scenario. This afforestation was allocated to central Brazil and the south of the FSU. The United States and European regions had large bio-crop production, predominantly in the south of the United States, but throughout all of Europe. This large bioenergy production was expected in the OECD countries because for bioenergy the CGE model assumes local production for local consumption.

We compare future land-use emissions and sinks estimated by the economic model and the land-use allocation model (see Fig. 9). There were similar trends at the global scale, but significantly different in some regions. The differences between the two models were mainly caused by the differences in carbon stock density and biomass growth rate of forests. For example, the Africa region and parts of Asia, such as India, had large differences in emissions because cropland expansion was allocated to areas where potential crop yields were high and forest carbon stocks were smaller compared to the values assumed in the economic model (see Fig. S8 in the Supplementary material for regional emissions).

4. Discussion

4.1. Interpretations

Our verification showed degree and cause of uncertainty which may occur in future projections within the range of changes seen in the past 45 years. Determining an uncertainty range in land use projections would improve the interpretation of model results and future land-use estimates in the assessment of policy and impacts for at least the next half a century. However, this result does not always guarantee the accuracy of estimates with large changes, as seen in the long-term scenario (i.e., to the end of this century), or stringent climate mitigation scenarios with dynamic land-use changes due to large-scale bio-energy use. Further work is needed to understand in more depth the driver of land use allocation and the causes of uncertainty to improve the land use projections for a longer term.

Since land-use is a main part of global environmental changes, downscaling future land-use projection estimated by the IAMs would expand the application possibility and meanings of the model integration. We expect this model to be useful to model integrations between ESMs and IAMs and further understand of interactions between human and global environments. Moreover, regional disaggregation in IAMs is an ongoing challenge in such assessments (Hasegawa et al., 2014) because the IAMs have been used to assess impacts of climate change and mitigation measures which have regional heterogeneity. For example, considering the climate change impacts on crop production at a gridded level might change the magnitude of the regional impacts on land use change, food price and risk of hunger while considering potential bioenergy production at gridded level could provide more useful information about climate mitigation effects on biodiversity.

4.2. Future challenges of land-use allocations

There are some challenges to be addressed in future study. With regard to the socioeconomic conditions as a driving force of the land-use, for example, accessibility to the market (for example, the spread of transport infrastructure such as roads and railways, distance to urban areas, and transportation costs) was not explicitly considered in this study because there was insufficient information regarding the historical dissemination of the transportation infrastructure, and the connection of consumption and production areas. The accessibility was implicitly considered in terms of population density. In addition, land-

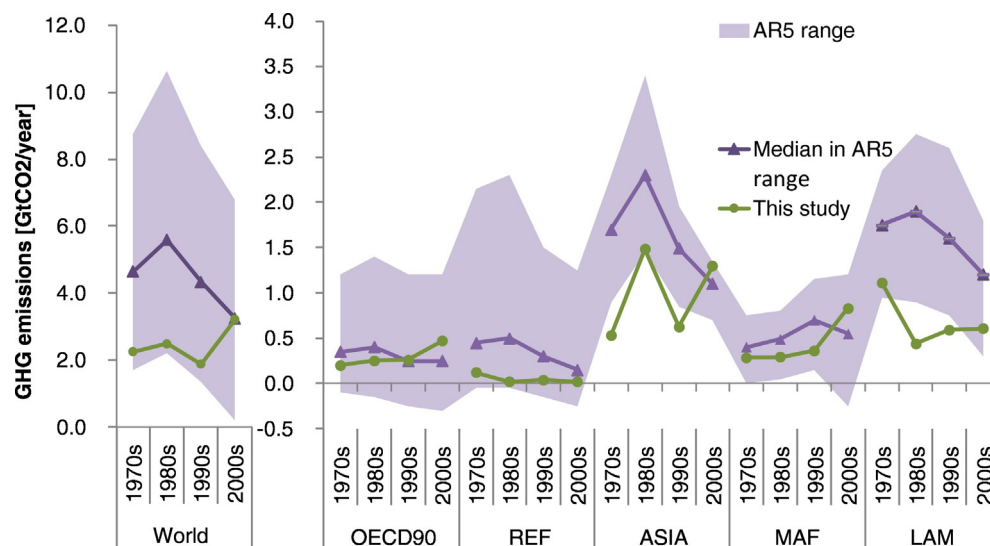


Fig. 6. Comparison of greenhouse gas emissions from land-use changes estimated in this study and values reported in the Fifth Assessment Report (AR5) of the United Nations Intergovernmental Panel on Climate Change (Smith et al., 2014). The range presented for the existing studies represents the uncertainty of the different models.

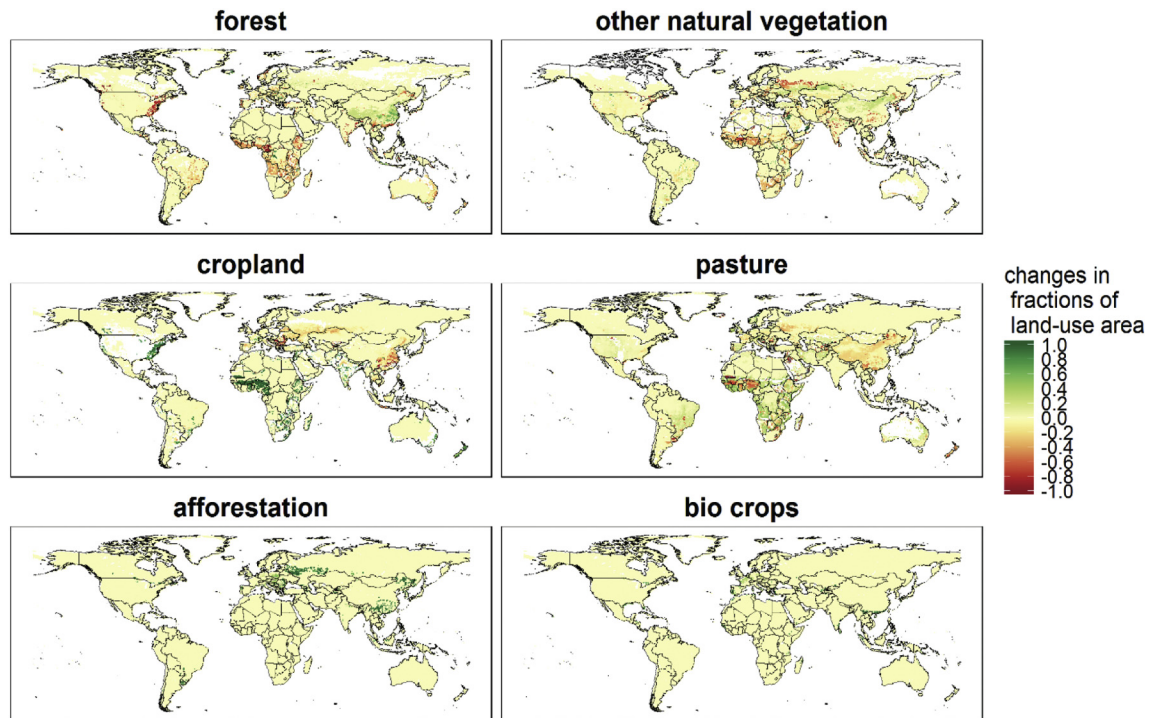


Fig. 7. Changes in the fractions of grid cell area occupied by each land-use category in 2100 from the 2005 level for the baseline scenario.

use policies and regulations might affect the land-use, but were not considered because such global data do not exist.

With respect to the biophysical factors, crop yield is a determinant of the land-use. The suitability of agricultural land, including soil conditions, water, and climate, were taken into account in crop models, and agricultural technology development was considered in AIM/CGE, whereas the following points were not considered in the crop yield and should be addressed in future studies. First, in model verification, irrigation ratio, which affects the suitability of agricultural land was fixed

to the current level because there were no data for historical irrigation spread. Second, land productivity generally decreases and production cost increases along with cropland expansion because of the effect of diminishing returns. Changes in productivity by land expansion across the grids were considered by using the spatial yield distribution, whereas effects that occurred within a grid were not explicitly considered. Third, the value of ecosystem services may be reflected in the actual land-use distribution. This study only considered the benefits from afforestation by uniformly assuming the value of forest restoration

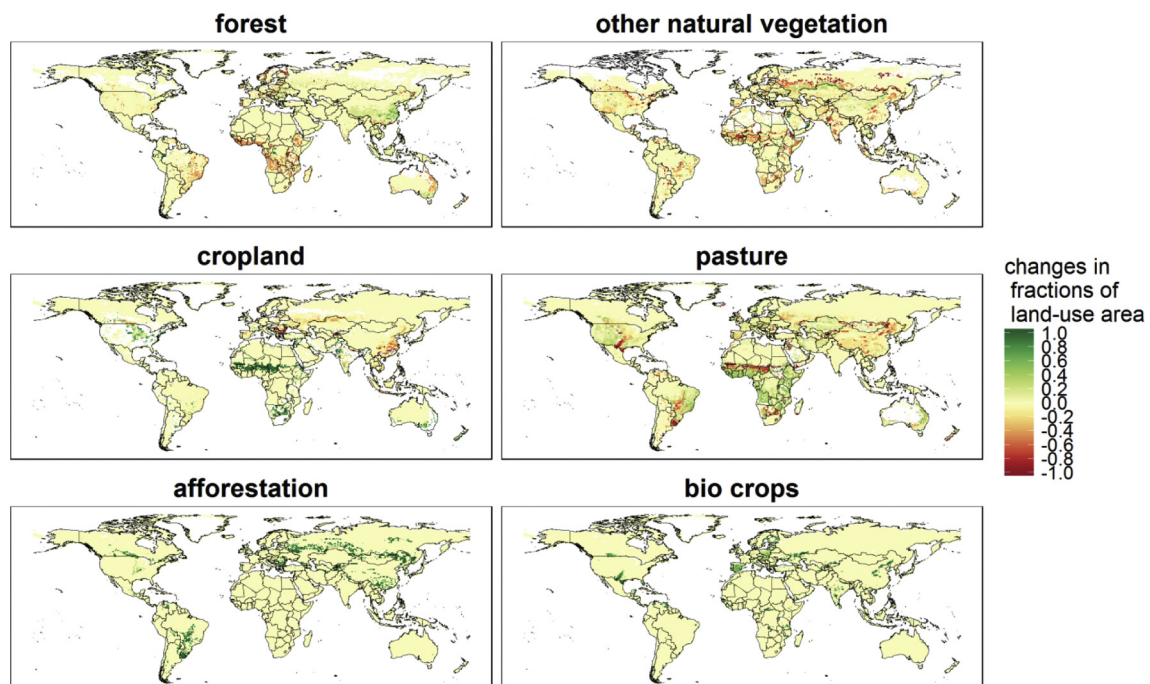


Fig. 8. Changes in the fractions of grid cell area occupied by each land-use category in 2100 from the level of 2005 for the mitigation scenario.

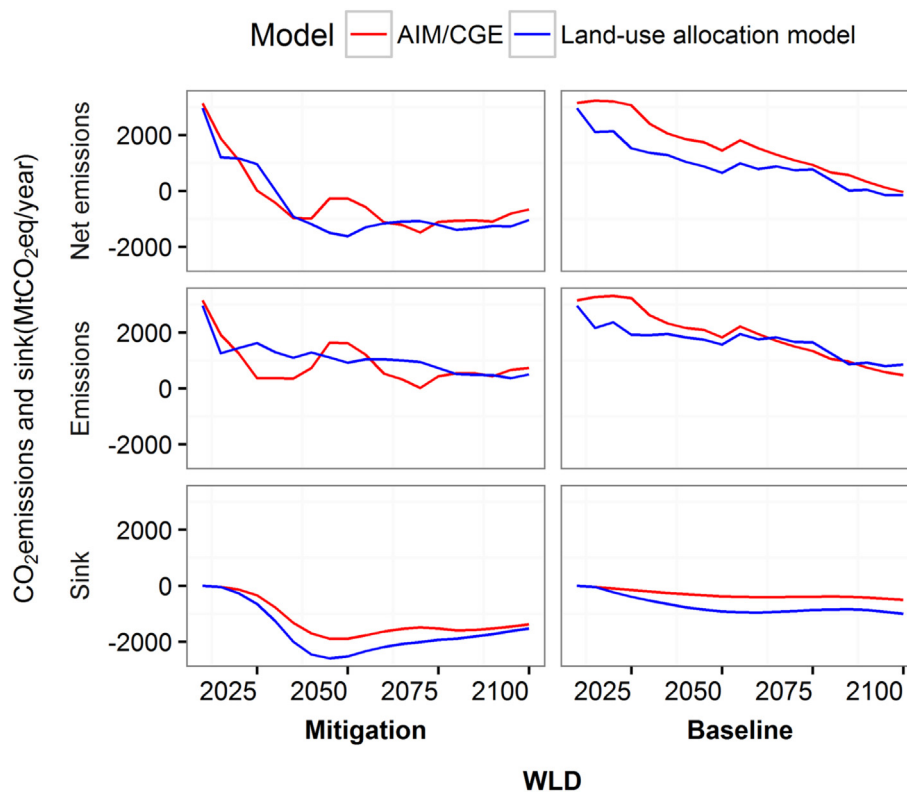


Fig. 9. Comparisons of CO₂ emissions and sinks estimated by the economic model and the land-use allocation model for the baseline and mitigation scenarios.

though the value lost due to deforestation and other destruction was not considered due to the difficulty of quantification.

5. Conclusions

We developed a land-use allocation model to downscale land-use data into a 0.5-degree resolution, and conducted a downscaling of future land-use scenarios estimated by an IAM (AIM/CGE) into a gridded level. To verify the model's downscaling technique, we applied the model to the past 45 years and evaluated the model agreement with existing studies. We found three features. First, the difference between the existing studies and our estimates of spatial distribution was relatively large where there had been a large historical cropland expansion. Second, the differences become larger over time, and the mean difference reached 0.18/grid for cropland and 0.11/grid for pasture land in the past 45 years. Third, we obtained a similar trend in global carbon emissions due to land-use changes, but there were regional differences between the estimates and values reported in existing studies.

As a result of the downscaling of the aggregated scenario, total carbon net emissions estimated by the land-use allocation model and the AIM/CGE model were comparable at the global scale, but there was discrepancy in regional scale. The regional differences were caused mainly by the spatial distribution of carbon stock density and the growth rate of forest biomass. For example in Sub-Saharan Africa and India, cropland expansion was allocated to an area with a small carbon stock density compared to the value assumed in AIM/CGE. The economic model contained a rough description of regional biophysical conditions due to regional aggregation, and did not capture such spatial distribution. This indicates that a framework combined with the land allocation model would enhance the spatial descriptions in economic models or IAMs and would help in assessing climate impacts on a wider spatial aspect such as biodiversity and water resource as well as designing effective adaptation and risk management strategies. To ease such further analysis, all data and methodology presented here is made available to the wider community.

Author contributions

TH, SF, and KT conceived and designed the research; TH and AI performed the experiments; TH, SF, KT and TM analyzed the data; TH, SF, AI and KT contributed to the writing of the manuscript.

Acknowledgements

This work was supported by the Research on Development of an Integrated Assessment Model incorporating Global-scale Climate Change Mitigation and Adaptation [Project Code S-14-5]; Japan Society for the Promotion of Science (JSPS) KAKENHI [Grant Number 15K16164 and 16K18177]; and the climate change research program of the National Institute for Environmental Studies [Project Code PJ1].

Appendix A. Supplementary data

Supplementary data to this article can be found online at <http://dx.doi.org/10.1016/j.scitotenv.2016.12.025>.

References

- Alexander, P., Prestele, R., Verburg, P.H., Arneith, A., Baranzelli, C., Batista e Silva, F., et al., 2016. Assessing uncertainties in land cover projections. *Glob. Chang. Biol.* (n/a-n/a).
- Bond-Lamberty, B., Calvin, K., Jones, A.D., Mao, J., Patel, P., Shi, X.Y., et al., 2014. On linking an Earth system model to the equilibrium carbon representation of an economically optimizing land use model. *Geosci. Model Dev.* 7, 2545–2555.
- Bryan, B.A., Nolan, M., McKellar, L., Connor, J.D., Newth, D., Harwood, T., et al., 2016. Land-use and sustainability under intersecting global change and domestic policy scenarios: trajectories for Australia to 2050. *Glob. Environ. Chang.* 38, 130–152.
- FAO, 2013. *FAOSTAT*, Rome, Italy.
- Fujimori, S., Masui, T., Matsuoka, Y., 2012. AIM/CGE [Basic] Manual. Discussion paper series Center for Social and Environmental Systems Research, NIES, Tsukuba, Japan.
- Fujimori, S., Hasegawa, T., Masui, T., Takahashi, K., 2014. Land use representation in a global CGE model for long-term simulation: CET vs. logit functions. *Food Sec.* 6, 685–699.
- Gao, L., Bryan, B.A., Nolan, M., Connor, J.D., Song, X., Zhao, G., 2016. Robust global sensitivity analysis under deep uncertainty via scenario analysis. *Environ. Model Softw.* 76, 154–166.

- Hasegawa, T., Fujimori, S., Shin, Y., Takahashi, K., Masui, T., Tanaka, A., 2014. Climate change impact and adaptation assessment on food consumption utilizing a new scenario framework. *Environ. Sci. Technol.* 48, 438–445.
- Hasegawa, T., Fujimori, S., Shin, Y., Tanaka, A., Takahashi, K., Masui, T., 2015. Consequence of climate mitigation on the risk of hunger. *Environ. Sci. Technol.* 49, 7245–7253.
- Hasegawa, T., Fujimori, S., Takahashi, K., Yokohata, T., Masui, T., 2016. Economic implications of climate change impacts on human health through undernourishment. *Clim. Chang.* 1–14.
- Havlik, P., Schneider, U.A., Schmid, E., Böttcher, H., Fritz, S., Skalský, R., et al., 2011. Global land-use implications of first and second generation biofuel targets. *Energy Policy* 39, 5690–5702.
- Havlik, P., Valin, H., Herrero, M., Obersteiner, M., Schmid, E., Rufino, M.C., et al., 2014. Climate change mitigation through livestock system transitions. *Proc. Natl. Acad. Sci.*
- Hibbard, K., Janetos, A., van Vuuren, D.P., Pongratz, J., Rose, S.K., Betts, R., et al., 2010. Research priorities in land use and land-cover change for the Earth system and integrated assessment modelling. *Int. J. Climatol.* 30, 2118–2128.
- Houghton, R., 2012. Carbon emissions and the drivers of deforestation and forest degradation in the tropics. *Curr. Opin. Environ. Sustain.* 4, 597–603.
- Hurt, G.C., Frolking, S., Fearon, M.G., Moore, B., Shevliakova, E., Malyshev, S., et al., 2006. The underpinnings of land-use history: three centuries of global gridded land-use transitions, wood-harvest activity, and resulting secondary lands. *Glob. Chang. Biol.* 12, 1208–1229.
- Hurt, G.C., Chini, L.P., Frolking, S., Betts, R.A., Feddema, J., Fischer, G., et al., 2011. Harmonization of land-use scenarios for the period 1500–2100: 600 years of global gridded annual land-use transitions, wood harvest, and resulting secondary lands. *Clim. Chang.* 109, 117–161.
- IPCC, 2006. In: Eggleston, H.S., Buendia, L., Miwa, K., Ngara, T., Tanabe, K. (Eds.), 2006 IPCC Guidelines for National Greenhouse Gas Inventories, Prepared by the National Greenhouse Gas Inventories Programme. IGES.
- IRF, 2009. World Road Statistics.
- Ito, A., Inatomi, M., 2012. Water-use efficiency of the terrestrial biosphere: a model analysis focusing on interactions between the global carbon and water cycles. *J. Hydrometeorol.* 13, 681–694.
- Jain, A.K., Meiyappan, P., Song, Y., House, J.I., 2013. CO₂ emissions from land-use change affected more by nitrogen cycle, than by the choice of land-cover data. *Glob. Chang. Biol.* 19, 2893–2906.
- Klein Goldewijk, K., Beusen, A., van Drecht, G., de Vos, M., 2011. The HYDE 3.1 spatially explicit database of human-induced global land-use change over the past 12,000 years. *Glob. Ecol. Biogeogr.* 20, 73–86.
- Kok, K., Farrow, A., Veldkamp, A., Verburg, P.H., 2001. A method and application of multi-scale validation in spatial land use models. *Agric. Ecosyst. Environ.* 85, 223–238.
- Letourneau, A., Verburg, P.H., Stehfest, E., 2012. A land-use systems approach to represent land-use dynamics at continental and global scales. *Environ. Model Softw.* 33, 61–79.
- Lotze-Campen, H., Popp, A., Beringer, T., Müller, C., Bondeau, A., Rost, S., et al., 2010. Scenarios of global bioenergy production: the trade-offs between agricultural expansion, intensification and trade. *Ecol. Model.* 221, 2188–2196.
- Masutomi, Y., Takahashi, K., Harasawa, H., Matsuoka, Y., 2009. Impact assessment of climate change on rice production in Asia in comprehensive consideration of process/parameter uncertainty in general circulation models. *Agric. Ecosyst. Environ.* 131, 281–291.
- Meiyappan, P., Dalton, M., O'Neill, B.C., Jain, A.K., 2014. Spatial modeling of agricultural land use change at global scale. *Ecol. Model.* 291, 152–174.
- Monfreda, C., Ramankutty, N., Foley, J.A., 2008. Farming the planet. Part 2: geographic distribution of crop areas, yields, physiological types, and net primary production in the year 2000. *Glob. Biogeochem. Cycles* 22.
- Nelson, G.C., Rosegrant, M.W., Koo, J., Robertson, R.D., Sulser, T., Zhu, T., et al., 2009. Climate change: impact on agriculture and costs of adaptation. Food Policy Report, Washington, D.C., p. 30
- Ramankutty, N., 2012. Global Cropland and Pasture Data from 1700–2007. Available online at [<http://www.geog.mcgill.ca/~nramankutty/Datasets/Datasets.html>] from the LUGE (Land Use and the Global Environment) Laboratory, Department of Geography, McGill University, Montreal, Quebec, Canada.
- Ramankutty, N., Foley, J.A., 2010. ISLSCP II Historical Croplands Cover, 1700–1992. ORNL Distributed Active Archive Center.
- Rosenzweig, C., Elliott, J., Deryng, D., Ruane, A.C., Müller, C., Arneth, A., et al., 2014. Assessing agricultural risks of climate change in the 21st century in a global gridded crop model intercomparison. *Proc. Natl. Acad. Sci.* 111, 3268–3273.
- Schaldach, R., Alcamo, J., Koch, J., Kölling, C., Lapola, D.M., Schüngel, J., et al., 2011. An integrated approach to modelling land-use change on continental and global scales. *Environ. Model Softw.* 26, 1041–1051.
- Smith, P.M.B., Ahmmed, H., Clark, H., Dong, H., Elsiddig, E.A., Haberl, H., Harper, R., House, J., Jafari, M., Masera, O., Mbow, C., Ravindranath, N.H., Rice, C.W., Robledo Abad, C., Romanovskaya, A., Sperling, F., Tubiello, F., 2014. Agriculture, Forestry and Other Land Use (AFOLU). In: Edenhofer, O., Pichs-Madruga, R., Sokona, Y., Farahani, E., Kadner, S., Seyboth, K., Adler, A., Baum, I., Brunner, S., Eickemeier, P., Kriemann, B., Savolainen, J., Schlömer, S., von Stechow, C., Zwickel, T., Minx, J.C. (Eds.), Climate Change 2014: Mitigation of Climate Change. Contribution of Working Group III to the Fifth Assessment Report of the Intergovernmental Panel on Climate Change. Cambridge University Press, Cambridge, United Kingdom and New York, NY, USA.
- Sohngen, B., Golub, A.A., Hertel, T.W., 2009. The Role of Forestry in Carbon Sequestration in General Equilibrium Models.
- Souty, F., Brunelle, T., Dumas, P., Dorin, B., Ciais, P., Crassous, R., et al., 2012. The Nexus Land-Use model version 1.0, an approach articulating biophysical potentials and economic dynamics to model competition for land-use. *Geosci. Model Dev.* 5, 1297–1322.
- UNEP-WCMC Ia, 2015. The World Database on Protected Areas (WDPA). [On-line], [May 2015 of the version downloaded], Available at: www.protectedplanet.net. UNEP-WCMC, Cambridge, UK.
- van Asselen, S., Verburg, P.H., 2013. Land cover change or land-use intensification: simulating land system change with a global-scale land change model. *Glob. Chang. Biol.* 19, 3648–3667.
- van Vuuren, D.P., Smith, S.J., Riahi, K., 2010. Downscaling socioeconomic and emissions scenarios for global environmental change research: A review. *Wiley Interdiscip. Rev. Clim. Chang.* 1, 393–404.
- Verburg, P.H., Schot, P.P., Dijst, M.J., Veldkamp, A., 2004. Land use change modelling: current practice and research priorities. *Geojournal* 61, 309–324.
- Wise, M., Calvin, K., 2011. GCAM3.0 Agriculture and Land Use: Technical Description of Modeling Approach. PNNL-20971. Pacific Northwest National Laboratory.
- WorldBank, 2014. In: WorldBank (Ed.), Unit Costs of Construction and Maintenance Works.